A Computational Neural Network Framework for Fractional-Order Modeling of Buruli Ulcer and Cholera: Insights into Microbial Genetics and Pathogenesis

Ghadeer Bukhari[1], Afaf S. Alwabli[1], S.I. Ali[2], Mohammed A. Balubaid[3], Jabr Aljedani[4], Ahmed Ramady[4], S. R. Mahmoud[4, *]

[1]Biological Sciences Department, College of Science & Arts, Rabigh Campus, King Abdulaziz University, Jeddah 21589, Saudi Arabia
[2]Department of Mathematics, Faculty of Science, Al-Azhar University, Nasr City 11884, Cairo, Egypt.
[3]Department of Industrial Engineering, Faculty of Engineering, King Abdulaziz University, Jeddah, Saudi Arabia.
[4]GRC Department, Applied College, King Abdulaziz University, Jeddah 21589, Saudi Arabia.
gfbukhari@kau.edu.sa , aalwabli@kau.edu.sa, *srhassan@kau.edu.sa

Abstract: This study develops a computational framework using a Levenberg-Marquardt backpropagation neural network (LMBNN) to solve the fractional-order Buruli ulcer (BU) and cholera model, integrating key aspects of microbial genetics and disease dynamics. The fractional-order model accounts for ten distinct categories, reflecting the nonlinear dynamics of infection, pathogen evolution, and host-pathogen interactions. Numerical solutions are derived using the stochastic LMBNN approach, supported by a dataset optimized with the Adam scheme. The data is partitioned into 76% for training and 12% each for validation and testing to minimize the Mean Square Error (MSE). The neural network employs a single layer with twelve neurons and a log-sigmoid activation function, offering precise approximations of disease dynamics. Validation against reference solutions shows negligible absolute error, confirming the solver's reliability. Statistical analyses further validate the model's robustness, making it a valuable tool for studying genetic resistance, microbial evolution, and the dynamics of infectious diseases.

Keywords: Cholera dynamics; Buruli ulcer; Neural networks; Fractional models; Levenberg-Marquardt; Epidemiology; Microbial genetics; Host-pathogen interaction.

1. Introduction

This research bridges the fields of microbiology and genetics by employing advanced fractional-order modeling and computational neural networks to analyze and predict the dynamics of infectious diseases such as Buruli ulcer and cholera. It provides a powerful framework for understanding pathogen behavior, environmental interactions, and the impact of antibiotics, while also integrating genetic factors that influence disease susceptibility and pathogen evolution. By combining genetic data with mathematical models, the study enhances

our ability to explore host-pathogen interactions, genetic predispositions, and the emergence of drug resistance. Furthermore, it supports genomic surveillance, precision medicine, and co-infection analysis, offering a comprehensive approach to tackling microbial infections and advancing public health interventions. This innovative methodology holds the potential to revolutionize the study of infectious diseases, addressing their complexity with interdisciplinary precision.

The construction of the mathematical systems for the epidemic diseases presents the nonlinear practice, which contains the infection dynamics in order to regulate the best possible controlling tactic [1–5]. The principle of fractional form is used to generalize the mathematical representations frequently built in ordinary or partial differential systems is now being investigated and is thought to be highly effective. Some of the diseases are mentioned with two modeling variables based on the problems of real world [1], modeling of Hepatitis E virus using the fractional kind of derivative [2], a novel fractional epidemic system [3], coronavirus system [4], and piecewise systems [5]. The better understanding of the infectious disease systems, the differential model should be formulated first in ordinary differential systems and then generalized into a fractional kind of models.

Mycobacterium ulcerans is the causative agent of Buruli ulcer (BU), sometimes referred to as necrotizing dermatitis, along with other transmissible diseases [6]. As things stand, the illness has been detected in a number of nations worldwide, with the tropical region having the highest rate of infection. Most West African nations, notably Cameroon, Cote d'Ivoire, Ghana, and Benin, which had the maximum occurrence; these nations accounted for about 80% of all cases that were reported worldwide [7]. Every endemic nation has foci where the disease is frequently observed. However, those who live in these environments are typically extremely poor and face significant obstacles in getting a chance at high-quality healthcare in their local areas [8].

The early detection of the illness and the administration of antibacterial agents, such as rifampicin and streptomycin for a minimum of two months are the only effective ways to stop the propagation of the BU contagion [9]. In a more advanced state, the lesion can require debridement or grafting, which will facilitate eventual and healing assist in avoiding abnormalities [10–12]. Long hospital stays are a hallmark of BU, which financially burden both the public and those being treated [13]. For example, the first comprehensive surveillance system implemented in Ghana discovered about 1200 BU cases between 1993 and 1998.

Unexpectedly, over 9000 instances were registered nationally between 2004 and 2014. Located in Ghana's Ashanti Province, the most prevalent area is Amansie West. It is closely linked to artisanal mining. Such communities frequently experience cholera outbreaks as a result of unprotected pit excavations. The illicit mining operations foster an atmosphere that is favorable to the growth of Mycobacterium ulcerans. This ultimately exposed children to poisons in the atmosphere and impairs their immune systems, which makes them more vulnerable to a variety of illnesses, most notably cholera because of inadequate sanitation brought on by the communities' extreme poverty [14].

J. Snow discovered cholera in the previous century, and that is how it is known today. In Sub-Saharan Africa, it is a common disease, although in West Africa Guinea is said to have been the first nation to report this illness [15]. The first recorded cholera's case reported on September 1, 1970, where a Togolese national received a diagnosis at Kotoka airport [16]. In Ghana, there were at least five significant cholera occurrences; the worst of them, with 243 recorded deaths, was in 2014. Approximately 3 to 5 million individuals are affected by the disease annually; African and Asian regions have seen the majority of instances [17]. The infection based on the cholera is linked with a serious diarrheal produced by the intestine infection along with the cholera of bacterium Vibrio. The state of infection is classified as mild, moderate, or severe, with approximately 20% of those infected displaying severe symptoms [18]. The symptoms of cholera include watery diarrhea and vomiting, which cause the affected person to run out of water and become exhausted [19]. As the intended course of therapy is not followed, the results are disastrous and the patient's life is in danger. Two established pathways have been identified for the cholera propagation: diseased people and the environment's aquatic reservoir [20]. Reducing the number of infections can be achieved by minimizing the environmental contaminants. In order to effectively stop the spread epidemic cholera over time, each community has to follow good sanitation and hygiene. Both diseases are quite widespread in Sub-Saharan Africa, especially in Ghana, as mining by artisans has left several unsanitary circumstances and stagnant water bodies that lead to cholera. Such mining villages typically have stationary bodies of water that are home to Mycobacterium ulcerans. Gaining a thorough grasp of the two illnesses is essential for emerging nations in West Africa, especially Ghana.

The mathematical modeling plays a vital role in order to better understand the disease spread dynamic and proper control mechanisms result in effective interference. Numerous investigations on the mathematical systems of cholera and BU have been conducted previously.

Some studies in the context of mathematical models are accessible in the scientific community to handle the complexity level of the cholera dynamics. For instance, the scientists created a mathematical form of the system, which is combined with the dynamic of cholera's environment into a traditional susceptible, infected and recovered (SIR) model [21]. The extension of the SIR system is presented by incorporating the hyper communicable pathogen nature [22]. The modification of the pathogen threshold based on the infection density is presented in [23] with particular consideration using in-reservoir pathogen dynamics and human–environment communication.

The cholera and BU disease model is considered one of the important system and various traditional techniques for the numerical solution of this model have been exploited. However, the execution of the stochastic framework based on the Levenberg-Marquardt backpropagation neural network (LMBNN) has never been implemented before to solve the fractional order BU and cholera model [24]. The fractional order derivatives are used to achieve more precise solutions of the model. In current decades, these solvers have been used in many applications, some of them are coronavirus model [25], HIV infection system [26], influenza disease model [27], food chain system [28], and breathing spreading epidemic model [29]. The mathematical form of the model is given in the system (1) [24].

$$\begin{cases} S_h'(t) = \pi_h + \psi R_c(t) + \phi R_b(t) + \theta R_{bc}(t) - \left(\beta_1 + \mu_h + \beta_h I_v(t)\right) S_h(t) \\ I_b'(t) = \beta_h I_v(t) S_h(t) - \beta_1 I_b(t) - \left(\mu_h + \eta + k\right) I_b(t) \\ I_c'(t) = \beta_1 S_h(t) - \beta_h I_c(t) I_v(t) - \left(l + \mu_h + \sigma\right) I_c(t) \\ D_{bc}'(t) = \beta_h I_c(t) I_v(t) + \beta_1 I_b(t) - \left(\varpi + \mu_h + \gamma + \delta\right) D_{bc}(t) \\ R_b'(t) = \eta I_b(t) - \varepsilon(\delta - 1) D_{bc}(t) - \left(\phi + \mu_h\right) R_b(t) \\ R_c'(t) = \sigma I_c(t) - (\varepsilon - 1)(\delta - 1) D_{bc}(t) - \left(\mu_h + \psi\right) R_c(t) \\ R_{bc}'(t) = \delta D_{bc}(t) - \left(\mu_h + \theta\right) R_{bc}(t) \\ B'(t) = \omega\left(\rho D_{bc}(t) + I_c\right) R_{bc}(t) - \mu_b B(t) \\ S_v'(t) = \pi_v - \beta_v \left(D_{bc}(t) + \mu_v + I_b(t)\right) S_v(t) \\ I_v'(t) = \beta_v \left(D_{bc}(t) + I_b(t)\right) S_v(t) - \mu_v I_v(t) \end{cases} \quad (1)$$

Where prime shows the derivative at time *t*, the detail of each parameter is described in Table 1.

Table 1: Description of each parameter used in the system (1)

Parameter	**Details**
Nh	Total human population
Sh	Susceptible human
Ib	Infected with BU
Ic	Infected
D_{bc}	Infected human with both cholera and BU
Rb	Human's recovery from BU
Rc	Human's recovery from cholera
R_{bc}	Human's recovery from both BU and cholera
Nv	Vector's population
Sv	Susceptible water bugs
Iv	Infected water bugs
β_1	Probability to obtain the infection by cholera
B	Bacteria population
π_h	Recruitment rate based on the healthy individuals
λ	Contact rate of Mycobacterium ulcerans based on the humans
l and γ	Death rates based on the cholera
β_h	Probability of human bugs receiving infection with BU
β_v	Probability of water bugs receiving infection with BU
β_h and k	Human's probability to get infection with BU
ϖ	BU related to the death rates
ω	Average influence of each cholera infected to the aquatic cholera's population
ϕ, ψ, θ	Rates of immunity waning
η, σ, δ	Rates of recovery
μ_h	Human's bugs mortality rate
μ_v	Water's bugs mortality rate
ρ	Modification parameter
β_v	probability of the Water bugs probability to get the BU infection
μ_b	Bacteria's death rate

The fractional kind of models is obtained by using the non-integer order derivatives and always considered complex nature. These derivatives obtained enormous attention due to frequent submissions in the area of science and engineering [30–32]. The fractional kind of derivatives represents a wider level of promises to design the model based on memory conditions. The

fractional kind of systems represent more accurate indications using the biological and physical fields and provide better performance using the power-law behavior, which is implemented in the engineering and natural systems. These derivatives are applied in the area of biology to examine the features of the rheological cell [33-34] and present a complex representation based on the physical systems [35-36]. The mathematical form of the fractional order BU and cholera model is shown as:

$$\begin{cases} S_h^{\Re}(t) = \pi_h + \psi R_c(t) + \phi R_b(t) + \theta R_{bc}(t) - \left(\beta_1 + \mu_h + \beta_h I_v(t)\right) S_h(t) \\ I_b^{\Re}(t) = \beta_h I_v(t) S_h(t) - \beta_1 I_b(t) - \left(\mu_h + \eta + k\right) I_b(t) \\ I_c^{\Re}(t) = \beta_1 S_h(t) - \beta_h I_c(t) I_v(t) - \left(l + \mu_h + \sigma\right) I_c(t) \\ D_{bc}^{\Re}(t) = \beta_h I_c(t) I_v(t) + \beta_1 I_b(t) - \left(\varpi + \mu_h + \gamma + \delta\right) D_{bc}(t) \\ R_b^{\Re}(t) = \eta I_b(t) - \varepsilon(\delta - 1) D_{bc}(t) - \left(\phi + \mu_h\right) R_b(t) \\ R_c^{\Re}(t) = \sigma I_c(t) - (\varepsilon - 1)(\delta - 1) D_{bc}(t) - \left(\mu_h + \psi\right) R_c(t) \\ R_{bc}^{\Re}(t) = \delta D_{bc}(t) - \left(\mu_h + \theta\right) R_{bc}(t) \\ B^{\Re}(t) = \omega\left(\rho D_{bc}(t) + I_c\right) R_{bc}(t) - \mu_b B(t) \\ S_v^{\Re}(t) = \pi_v - \beta_v \left(D_{bc}(t) + \mu_v + I_b(t)\right) S_v(t) \\ I_v^{\Re}(t) = \beta_v \left(D_{bc}(t) + I_b(t)\right) S_v(t) - \mu_v I_v(t) \end{cases} \tag{2}$$

Where $\Re$ represent the fractional order Caputo derivative that exist between 0 and 1. The novel features of current work are presented as:

- A design of stochastic paradigms is presented to solve the fractional order BU and cholera mathematical model.
- The fractional kind of derivatives provides more consistent results as compared to integer order.
- Three different cases based on the fractional order derivative values have been used to solve the model.
- The principles based on certification, testing, and training are functional to regulate the capability of the Adams method to create a dataset.
- The scheme correctness is perceived through the negligible absolute error (AE) and result's comparison.

The remaining parts of this work are given as: The stochastic approach is constructed in Section 2, the model's output are shown in Section 3, whereas the conclusions are drawn in Section 4.

2. Proposed LMBNN procedure

This section presents the stochastic computing structure and the scheme's execution. The proposed scheme is implemented to train the neural networks in order to solve the fractional kind of BU and cholera model. The implementation of this approach is mostly applied to solve the nonlinear systems for adjusting the network's weights in order to obtain the best values of the fitness. A neural network structure based is suggested to achieve the nonlinear relationship in the target performances along with input topographies. The system framework keeps a hidden, input, and output structure of the layers. The neural network's weights are adjusted, and the dataset is used to be trained through the inputs as well as outputs. The training data is fed into the process of iteration using the LMBNN. The designed LMBNN is generally applied to present the solutions of the nonlinear regression systems and curve fitting because of the elements of gradient descent and the Gauss-Newton approach. Fig. 1 presents the description of the fractional BU and cholera model. In the first part of Fig. 1, the mathematical model based on each class is presented, the procedure of reference solution and the detail of the proposed solution is described in the second part of Fig. 1, while the obtained results through the designed structure for the fractional BU and cholera model are presented in the last half of the Fig. 1. The scheme performances to solve the fractional BU and cholera model are described based on the 'nftool' command, which is a one of the optimization schemes in the "MATLAB" software, a structure of the layer, epochs, tolerance10^{-08}, *n*-folded cross authentication, 0.01 step size, twelve neurons, LMBNN procedure, while the activation function is used as log-sigmoid in this study. A dataset is applied to reduce the mean square error (MSE) by splitting the statics 12% for both endorsement and testing, while 76% is applied for training in order to solve the BU and cholera model.

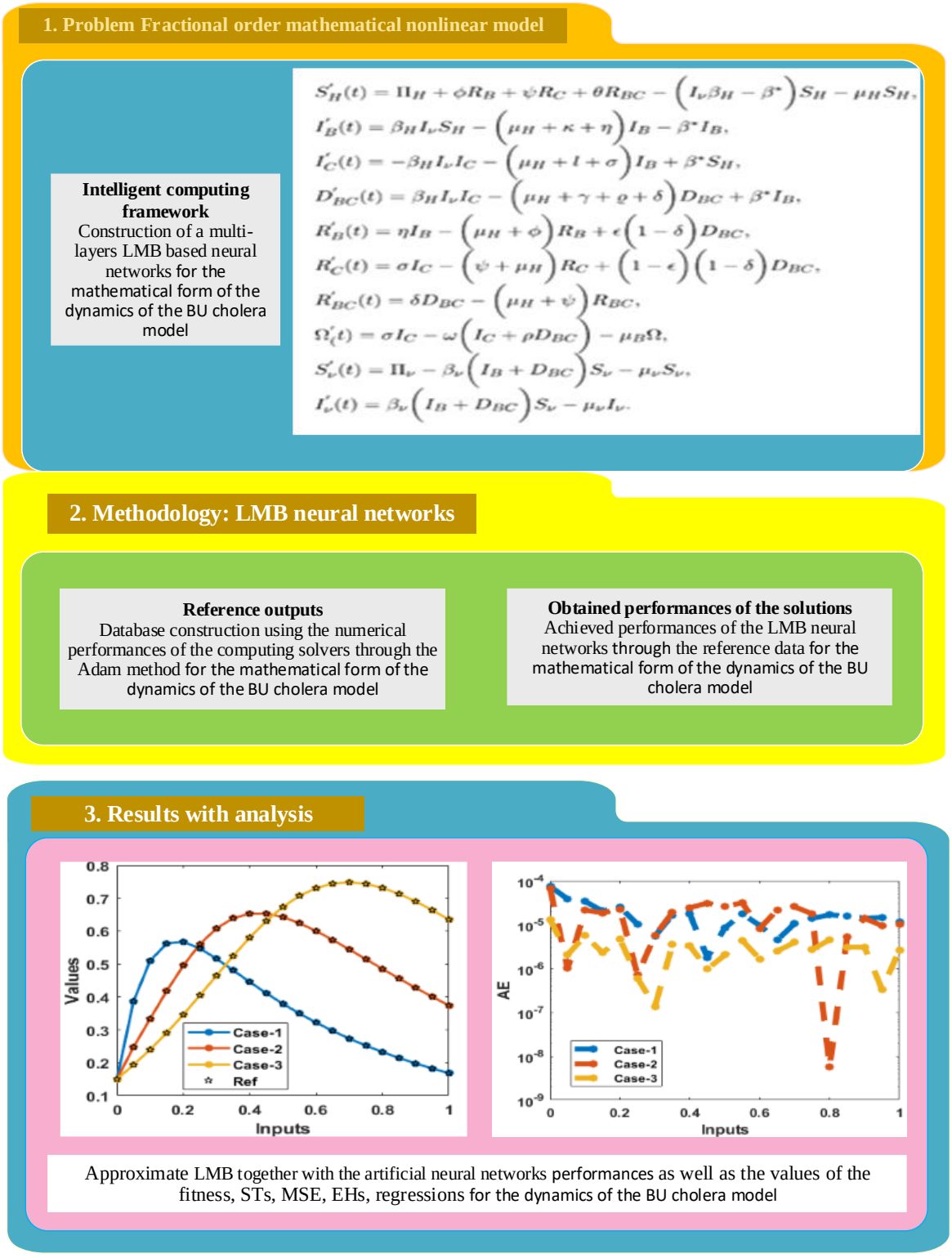

Figure 1: Workflow illustration to solve the fractional BU and cholera mathematical model.

The process of LMBNN approach is implemented to solve the fractional BU and cholera mathematical model is illustrated in Fig. 2 by using twelve numbers of neurons, which are validated through the optimal performances of overfitting or underfitting based on the

corroboration and training statics at epochs 33, 28 and 33. The performance of the scheme can be obtained better by taking higher numbers of neurons, but in this case the complexity cost gets high and overfitting can be performed, while to go against it the underfitting or premature results can be achieved by taking small neurons. For the lesser training values, i.e., 44 % to 55 %, the increment is performed in MSE and poor observations have been assessed normally. In the disparities of this, the training is used around 76%, while 12% for both endorsement and testing. While the computing strength solver is not severely documented using the unbiased data to choose the targets. Fig. 2 performs the layer structure to represent the solutions of the fractional BU and cholera mathematical model.

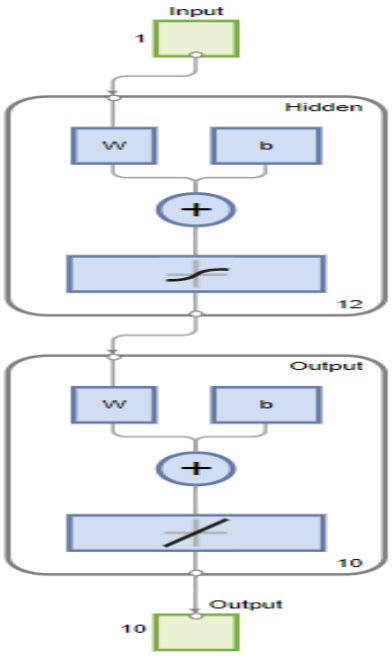

Figure 2: A design of the layers to solve the BU and cholera model

3. Numerical solutions

This section represents the calculated outcomes based on the BU and cholera model by applying the procedure of LMBNN. The numerical results of the system (2) are provided by choosing the values of the parameter as $\pi_h = 0.1$, $\phi = 0.12$, $\psi = 0.14$, $\theta = 0.16$, $\mu_h = 0.18$, $\beta_h = 0.2$, $\beta_1 = 0.26$, $\eta = 0.24$, $k = 0.22$, $l = 0.3$, $\sigma = 0.28$, $\gamma = 0.32$, $\delta = 0.36$, $\varpi = 0.34$, $\varepsilon = 0.38$, $\omega = 0.42$, $\mu_b = 0.4$, $\pi_v = 0.46$, $\mu_v = 0.5$, $\beta_v = 0.48$, $\rho = 0.4$ and the initial conditions are selected as $S_h(0) = 0.1$, $I_b(0) = 0.15$, $I_c(0) = 0.2$, $D_{bc}(0) = 0.25$, $R_b(0) = 0.3$,

$R_c(0) = 0.35$, $R_{bc}(0) = 0.4$, $B(0) = 0.45$, $S_v(0) = 0.5$ and $I_v(0) = 0.55$. Three cases have been derived based on the fractional order values, which are selected as 0.5, 0.7 and 0.9.

The numerical performances based on the fractional BU and cholera model are presented by applying the procedures of artificial neural networks. The graphical depictions to solve the BU and cholera model are provided in Fig. 3 to 7. Fig. 3 presents the best verification and a gradient for the fractional BU and cholera model that have been obtained through the proposed stochastic scheme for solving the fractional BU and cholera model. Fig. 3 (a to c) presents the obtained performances through MSE, which are reported based on the best curves, endorsement, and training, while the gradient for each case of the BU and cholera model are presented in Figs. 3(d–f). The best performances of the fractional BU and cholera model are illustrated at epochs 33, 28 and 33 that are shown as 2.5935×10^{-10}, 6.458×10^{-10} and 4.3858×10^{-11}. The gradient is performed through the LMBNN approach for fractional BU and cholera model is depicted as 9.5628×10^{-08}, 9.7781×10^{-08}, and 9.913×10^{-08} for case 1 to 3. These representations designate the outputs of the fractional BU and the cholera model in order to check the exactness, accuracy and convergence. Fig. 4(a to c) designates the representations of the fitting curve values to solve the fractional BU and cholera model. The error histogram (EH) is shown in Fig. 4(d to f) that is observed as 3.39×10^{-05}, 2.42×10^{-05} and 7.10×10^{-07} for variation 1 to 3 to solve the fractional BU and cholera model. The plots of the correlation are illustrated in Figs. (5 to 7) to solve the fractional BU and cholera model by applying the designed stochastic scheme. R^2 represents the coefficient determination that is 1 for variation 1 to 3 of the fractional BU and cholera model. Table 2 is designed based on the convergence by applying the training, endorsement, complexity, epochs, backpropagation, and testing.

Table 1: MSE for solving the fractional BU and cholera model.

Variant	MSE			Performance	Gradient	Mu	Epoch	Time
	Testing	Training	Validation					
I	3.3×10^{-10}	2.4×10^{-09}	2.5×10^{-10}	2.14×10^{-09}	9.56×10^{-07}	1×10^{-10}	33	3
2	5.8×10^{-10}	1.2×10^{-09}	6.4×10^{-10}	8.44×10^{-10}	9.78×10^{-08}	1×10^{-10}	28	2
3	1.9×10^{-11}	4.4×10^{-11}	4.3×10^{-11}	4.47×10^{-11}	9.01×10^{-08}	1×10^{-11}	33	2

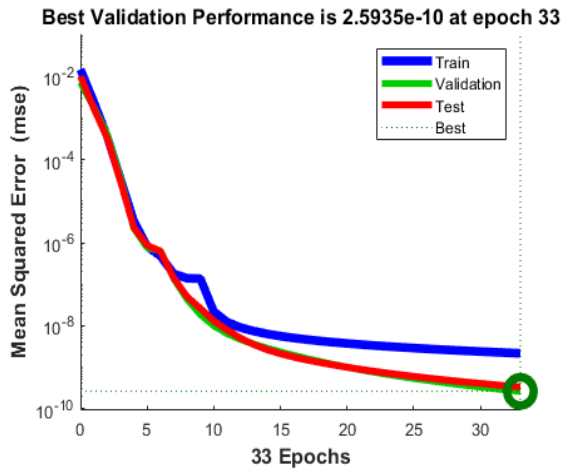

(a) Validation performances for case 1

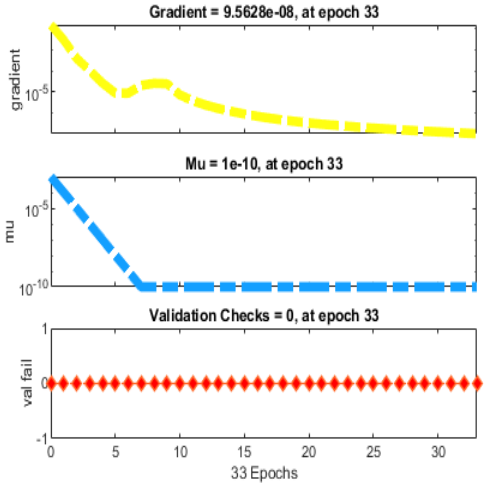

(d) Gradient for case 1

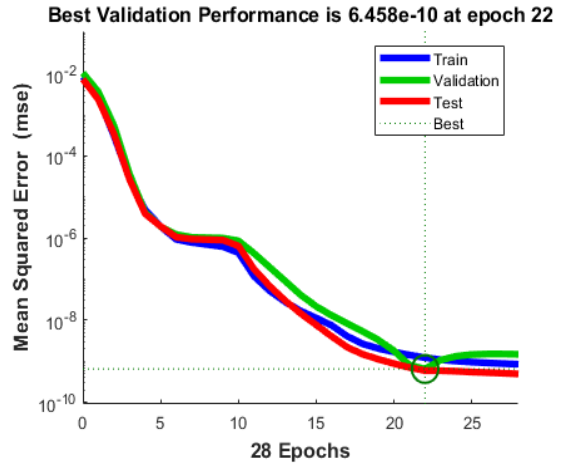

(b) Validation performances for case 2

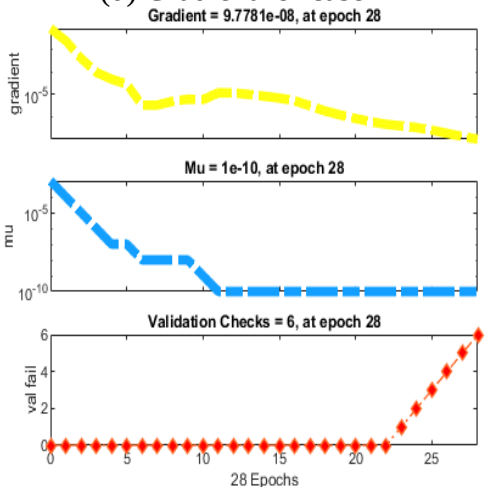

(e) Gradient for case 2

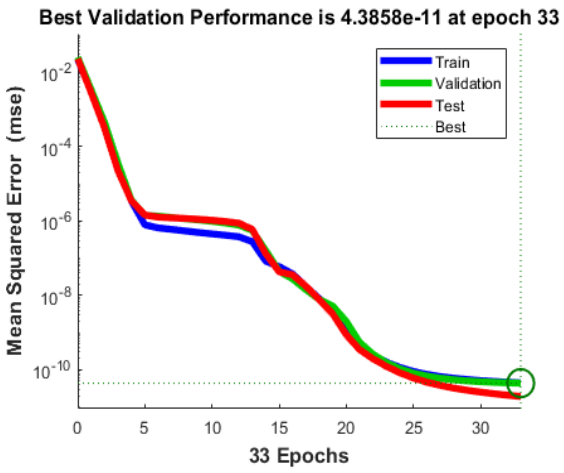

(c) Validation performances for case 3

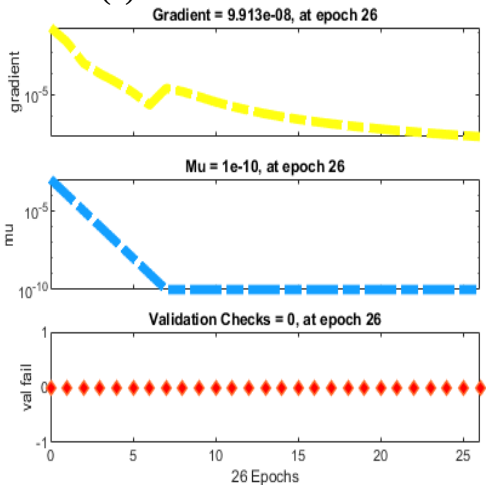

(f) Gradient for case 3

Figure 3: Best verification and gradient for the fractional BU and cholera model

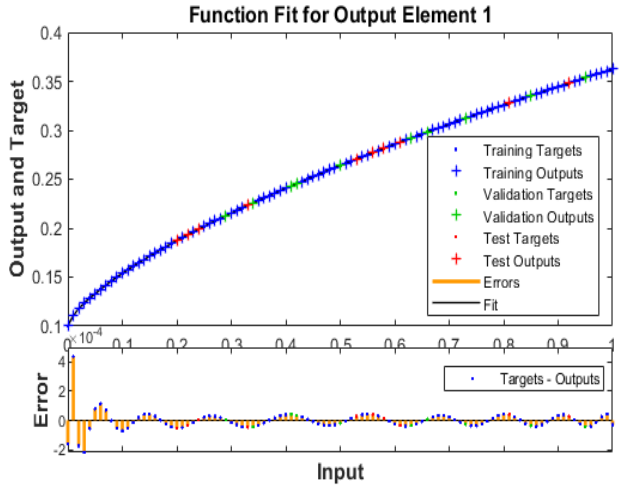

(a) Fun. Fit for variation 1

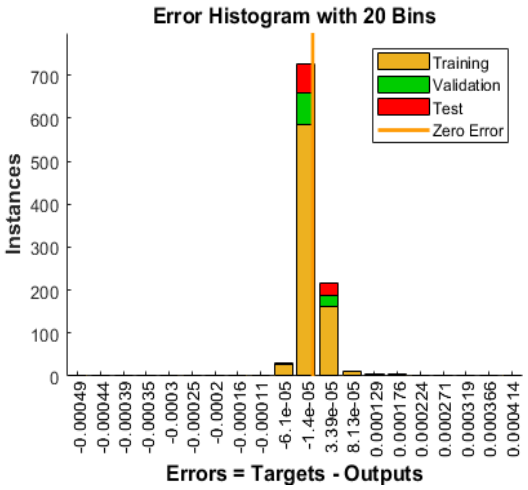

(d) EH for variation 1

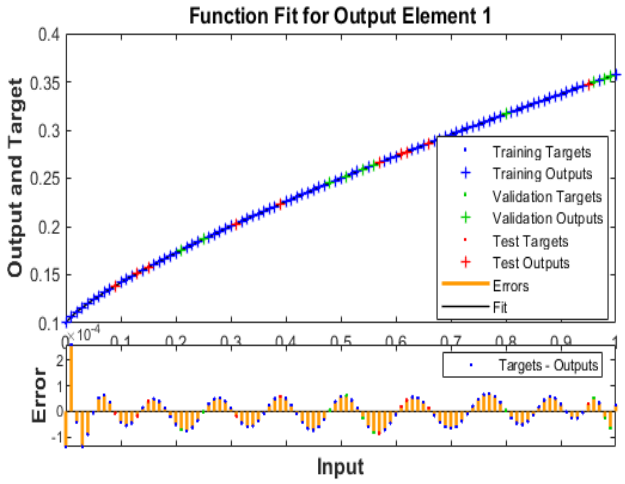

(b) Fun. Fit for variation 2

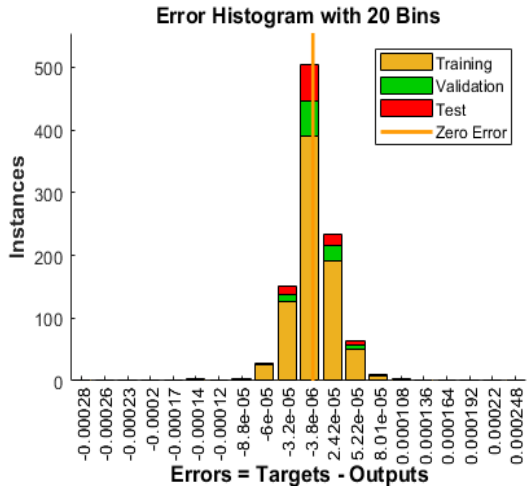

(e) EH for variation 2

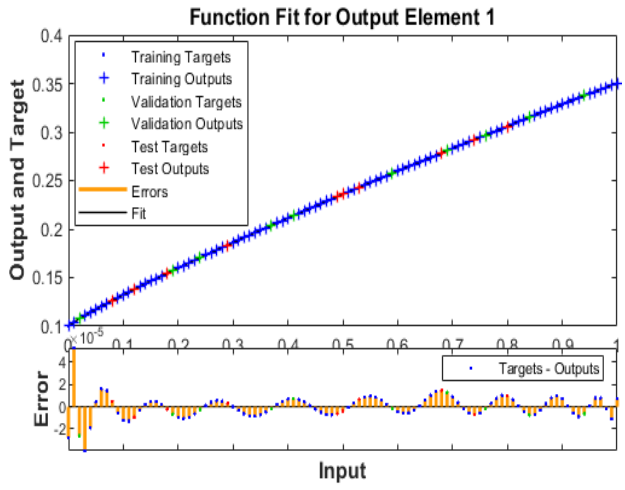

(c) Fun. Fit for variation 3

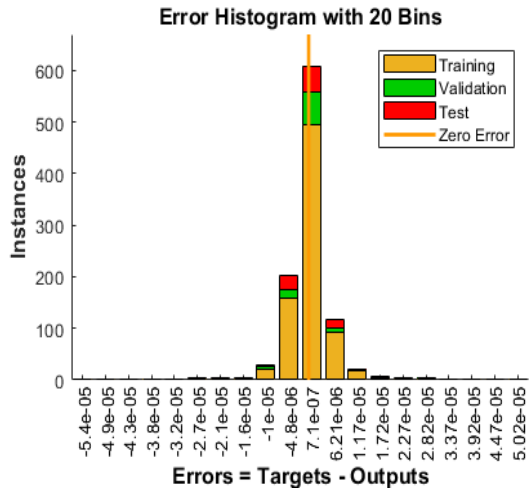

(f) EH for variation 3

Figure 4: Func. Fit and EH for each variation for the fractional BU and cholera model.

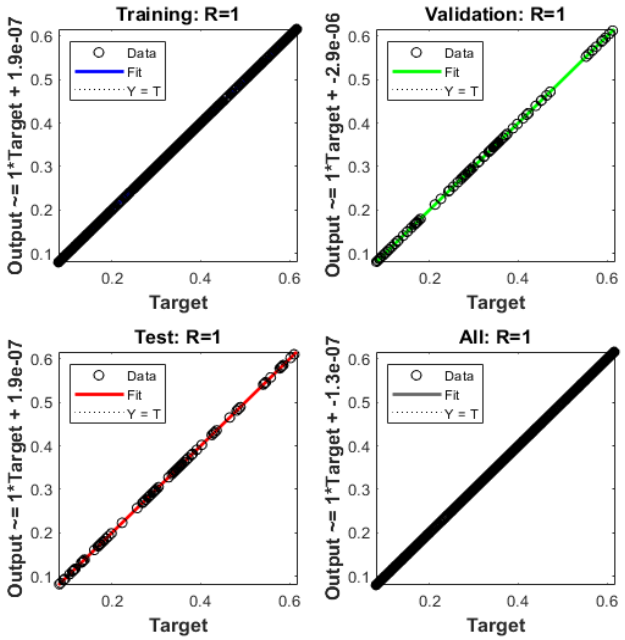

Figure 5: Regression for case 1 of the fractional BU and cholera model

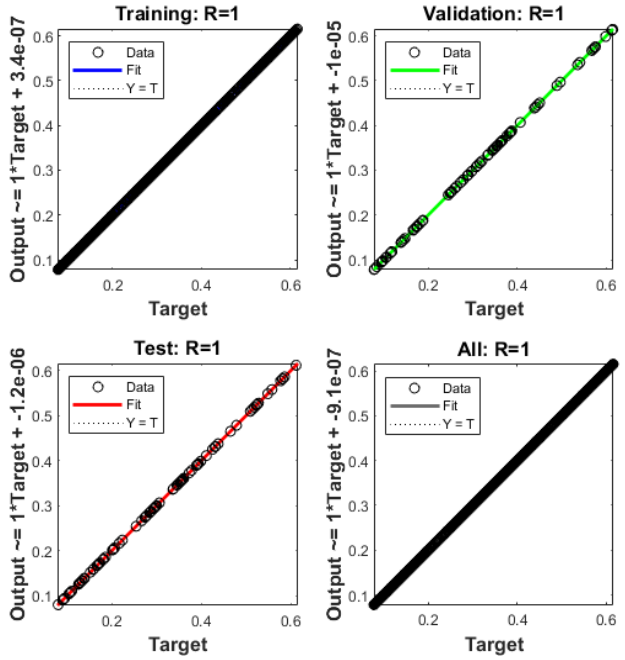

Figure 6: Regression for case 2 of the fractional BU and cholera model

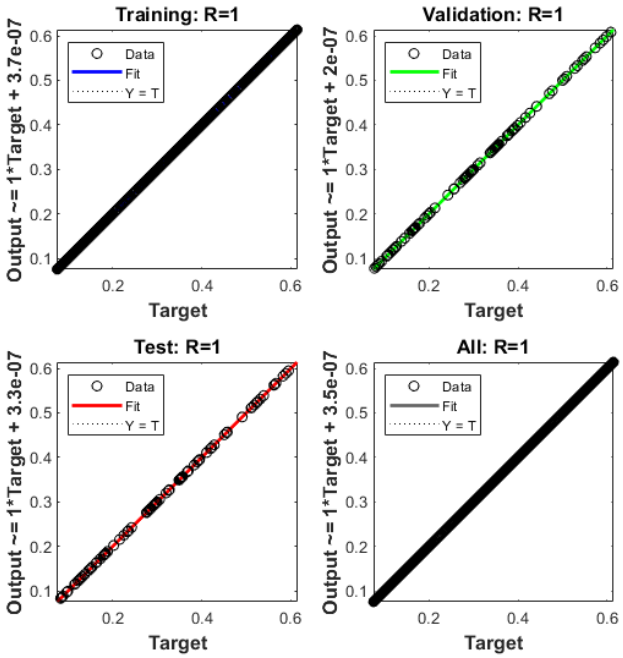

Figure 7: Regression for case 3 of the fractional BU and cholera model

For the solution of the fractional BU and cholera model based cases 1 to 3, the illustrations of the result comparisons and AE are shown in Figs. 8 and 9. The calculated and source outputs of the fractional BU and cholera model are depicted in Fig. 8 and the performances of the results designate the overlapping. These matching perform the correctness of the designed scheme to solve the fractional BU and cholera model. Fig. 9 provides the AE illustrations for each class of the fractional BU and cholera system. For the parameter $S_h(t)$, the AE are 10^{-04} to 10^{-06} for case 1 and 2, and 10^{-05} to 10^{-08} for case 3. For the class $I_b(t)$, these values are reported as 10^{-05} to 10^{-06}, 10^{-05} to 10^{-07} and 10^{-06} to 10^{-07} for respected BU and cholera model's cases. For $I_c(t)$, these performances are measured 10^{-05} to 10^{-07}, 10^{-05} to 10^{-08} and 10^{-06} to 10^{-08} for fractional BU and cholera model's case 1 to 3. The AE for the category $D_{bc}(t)$ are measured around 10^{-04} to 10^{-06} for case 1, 10^{-04} to 10^{-07} for case 2 and 10^{-05} to 10^{-08} for case 3. For class $R_b(t)$, these performances are shown as 10^{-05} to 10^{-06}, 10^{-05} to 10^{-07} and 10^{-06} to 10^{-07}. For $R_c(t)$, the AE for each case of the model are reported as 10^{-05} to 10^{-07}. For $R_{bc}(t)$, the AE performances are presented as 10^{-05} to 10^{-06} for first two cases and 10^{-06} to 10^{-07} for the third case. For $B(t)$, these values lie in the ranges of 10^{-04} to 10^{-07} for variation 1 to 3, while for the categories $S_v(t)$ and $I_v(t)$, these values are reported as 10^{-04} to 10^{-07} for each case of the model. These negligible performances of the AE designate the accuracy of the stochastic designed scheme for solving the fractional BU and cholera mathematical model.

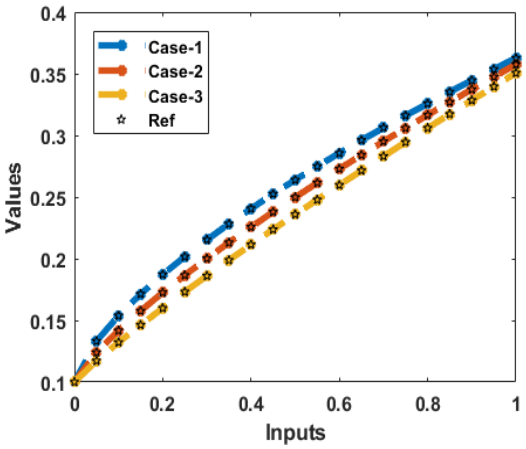

(a) Results: $S_h(t)$

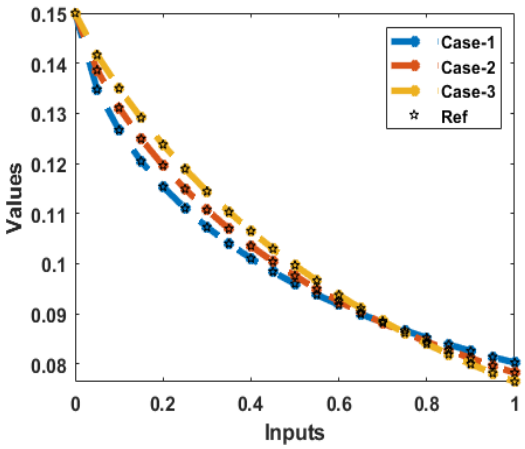

(b) Results: $I_b(t)$

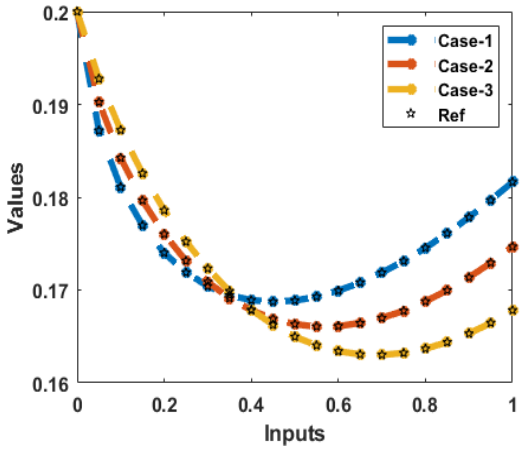

(c) Results: $I_c(t)$

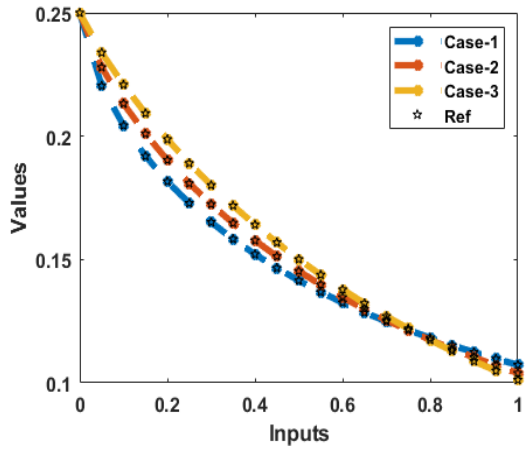

(d) Results: $D_{bc}(t)$

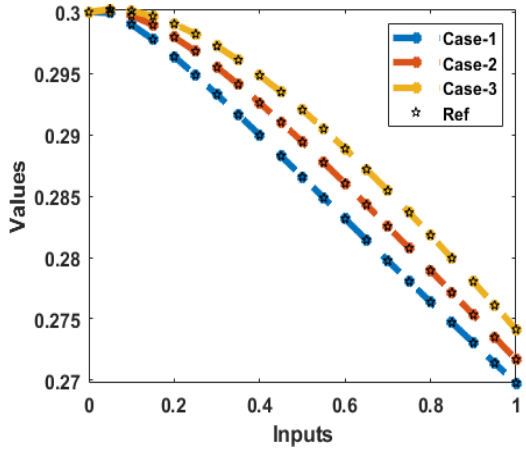

(e) Results: $R_b(t)$

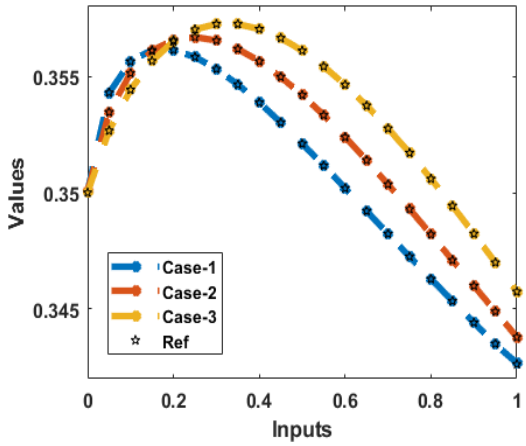

(f) Results: $R_c(t)$

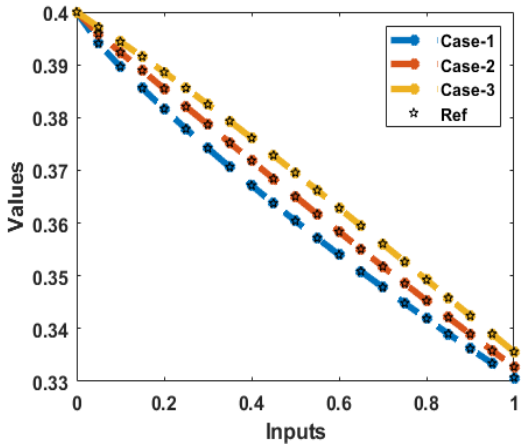

(g) Results: $R_{bc}(t)$

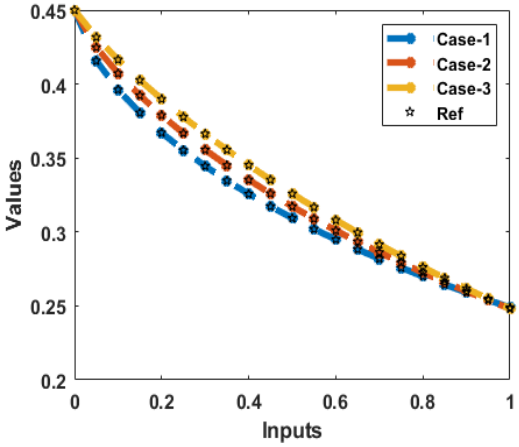

(h) Results: $B(t)$

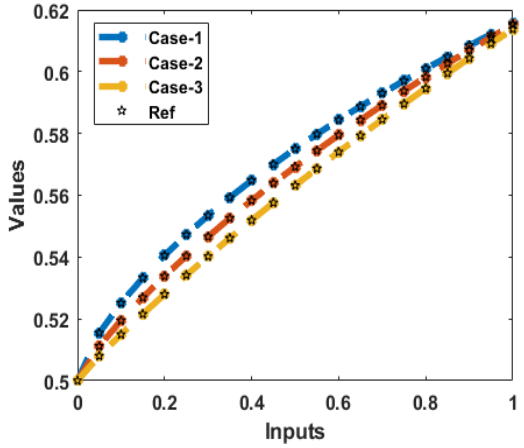

(i) Results: $S_v(t)$

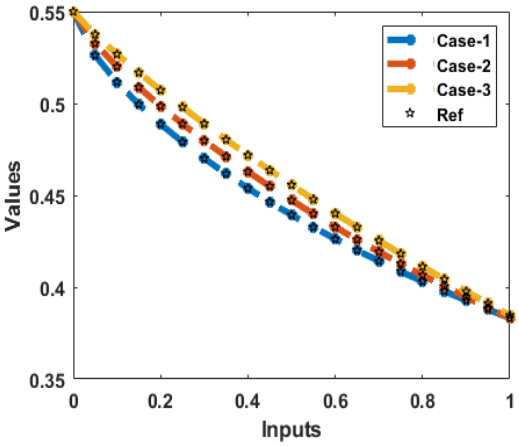

(j) Results: $I_v(t)$

Figure 8: Comparison of the outputs for solving the BU and cholera model

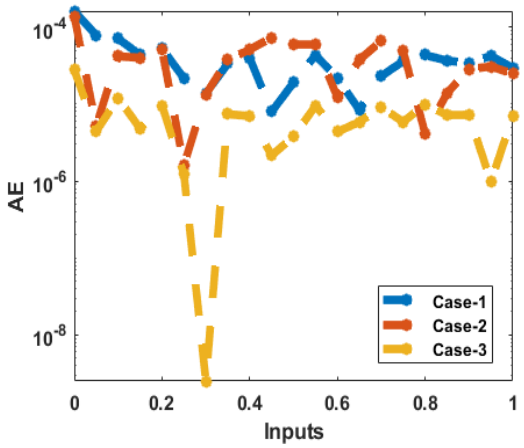

(a) Results: $S_h(t)$

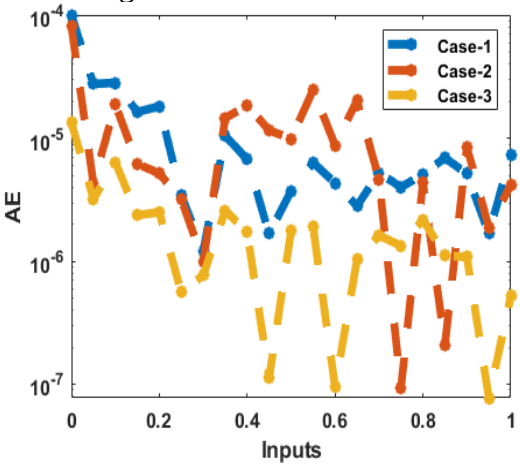

(b) Results: $I_b(t)$

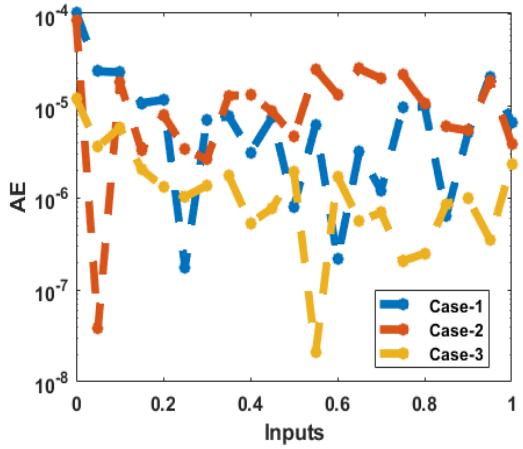

(c) AE: $I_c(t)$

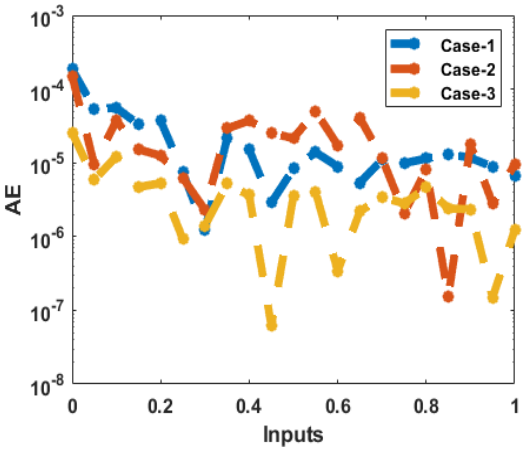

(d) AE: $D_{bc}(t)$

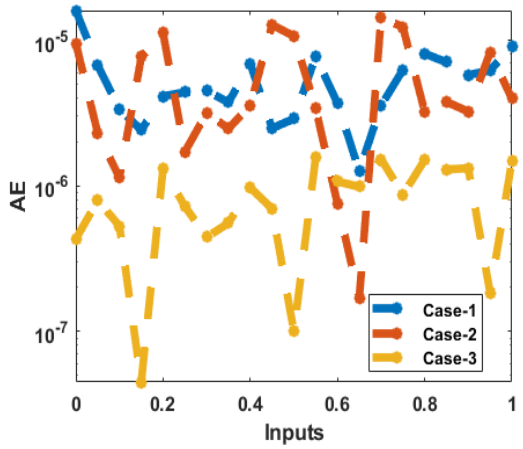

(e) AE: $R_b(t)$

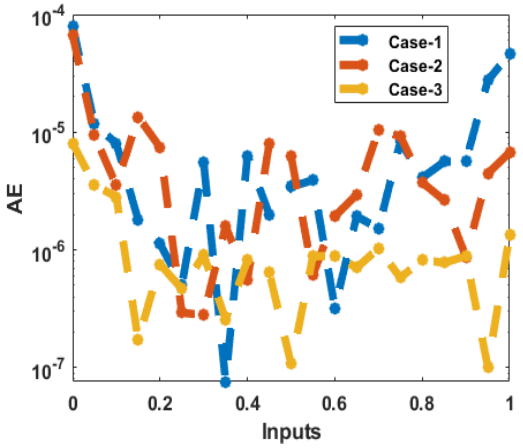

(f) AE: $R_c(t)$

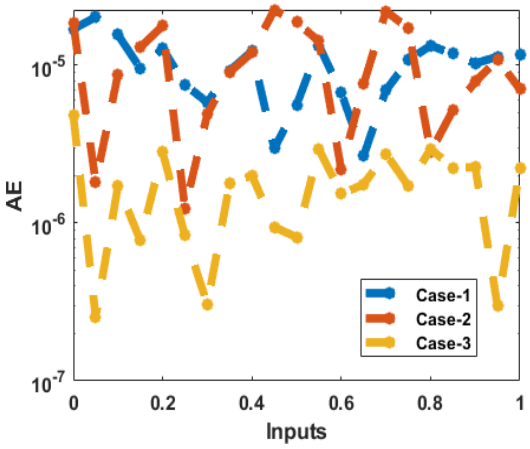

(g) AE: $R_{bc}(t)$

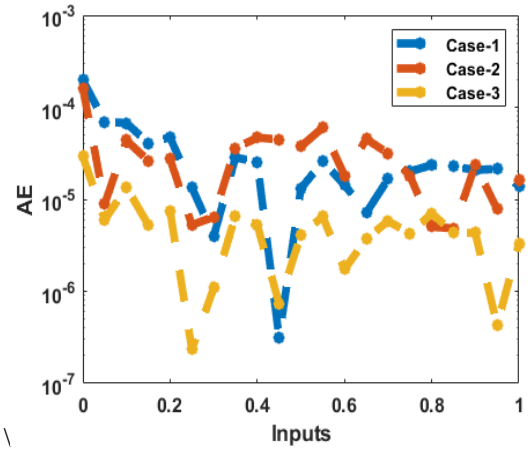

(h) AE: $B(t)$

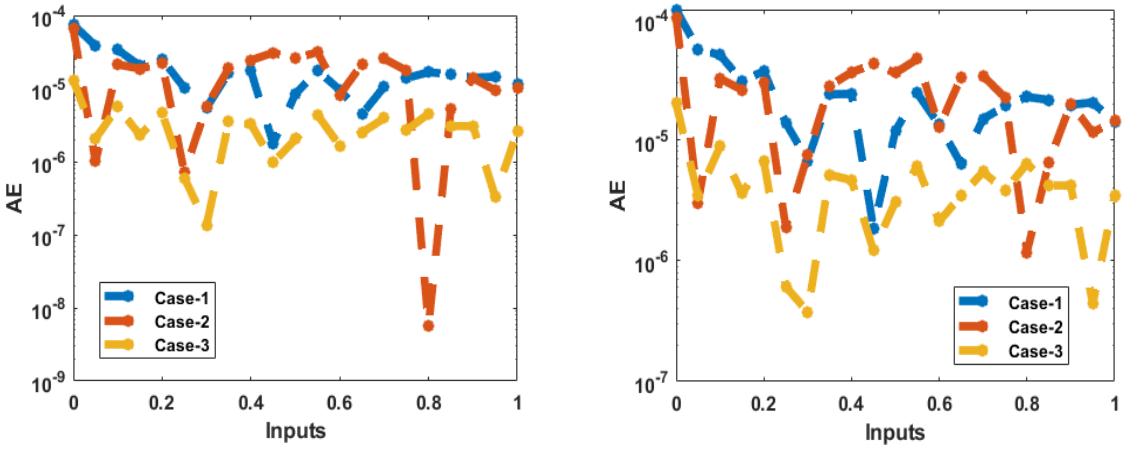

(i) AE: $S_v(t)$ (j) AE: $I_v(t)$

Figure 9: The values of the AE for each case of the BU and cholera model

Finally, the developed computational neural network framework for fractional-order modeling of Buruli ulcer and cholera provides a novel methodology for studying infectious disease dynamics with a focus on microbial genetics and host-pathogen interactions. The integration of fractional-order systems enhances the understanding of disease progression and the impact of genetic factors on pathogenesis and drug resistance. By building on the foundational principles of mechanical and mathematical modeling applied in diverse biological contexts, such as the nanoscale mechanical behavior of protein microtubules [37-39], thermal stress effects on cellular structures [40], and biomechanical applications in mosquito control [44-46], this research bridges interdisciplinary fields to address the complexity of infectious diseases. The insights drawn from this framework, supported by robust validation techniques and computational accuracy, align with the broader efforts in applying mathematical models to biological systems, such as tumor growth and shear deformation theories [42-43], enabling precise control strategies for disease management and public health interventions. Future applications may extend these models to explore genetic mutations, pathogen evolution, and co-infection scenarios, building upon the success of fractional-order and neural network-based approaches [41].

4. Conclusions

This study implemented a stochastic Levenberg-Marquardt backpropagation neural network (LMBNN) to numerically solve the fractional-order Buruli ulcer (BU) and cholera model, which incorporates ten distinct categories. The research highlights the intersection of computational methods, microbiology, and genetics, with the following key conclusions:

- The fractional-order model provides more accurate and biologically relevant insights into the dynamics of Mycobacterium ulcerans (BU) and Vibrio cholerae (cholera) compared to traditional integer-order models.
- The solver effectively integrates microbial and genetic parameters, such as host-pathogen interactions and genetic resistance dynamics, offering a robust framework for understanding disease progression and control.
- A well-structured dataset, optimized using the Adam solver, achieved high accuracy by splitting data into 76% training, 12% validation, and 12% testing to minimize the Mean Square Error (MSE).

- The neural network's structure, featuring twelve neurons, a log-sigmoid activation function, and n-fold cross-validation, demonstrated excellent performance, achieving a coefficient of determination (R^2) of 1 for variations of the model, signifying perfect prediction accuracy.
- The solver's accuracy was validated through statistical presentations, showing negligible absolute errors and reliable overlapping of results with reference solutions.
- This approach provides a computational framework for studying the genetic factors influencing pathogen evolution, host immune responses, and drug resistance in microbial systems.

Future applications of this methodology include solving complex nonlinear models in microbiology and genetics, such as pathogen evolution, genetic mutations, and host-pathogen dynamics in fluid and epidemic systems.

Acknowledgment

This project was funded by the Deanship of Scientific Research (DSR) at King Abdulaziz University, Jeddah, under grant no. (GPIP: 2034-665-2024). The authors, therefore, acknowledge with thanks DSR for technical and financial support.

References

[1] Owolabi KM, Hammouch Z. Mathematical modeling and analysis of two-variable system with noninteger-order derivative. Chaos 2019; 29(1):013145.
[2] Khan MA, Hammouch Z, Baleanu D. Modeling the dynamics of hepatitis E via the Caputo–Fabrizio derivative. Math Model Nat Phenom 2019; 14.
[3] Singh J, Kumar D, Hammouch Z, Atangana A. A fractional epidemiological model for computer viruses pertaining to a new fractional derivative. Appl Math Comput 2018; 316:504–15.
[4] Atangana A, Araz SI. Modeling third waves of Covid-19 spread with piecewise differential and integral operators: Turkey, Spain and Czechia. 2021, medRxiv.
[5] Atangana, A. and Araz, S.İ., 2021. New concept in calculus: Piecewise differential and integral operators. Chaos, Solitons & Fractals, 145, p.110638.
[6] To, K.K. and Yuen, K.Y., 2012. In memory of Patrick Manson, founding father of tropical medicine and the discovery of vector-borne infections. Emerging Microbes & Infections, 1(1), pp.1-7.
[7] Hennigan, C.E., Myers, L. and Ferris, M.J., 2013. Environmental distribution and seasonal prevalence of Mycobacterium ulcerans in Southern Louisiana. Applied and environmental microbiology, 79(8), pp.2648-2656.
[8] Kofie, R.Y., Attua, E.M. and Nabila, J.S., 2008. Poverty and socio-economic consequences of Buruli ulcer (Mycobacterium ulcerans) in the Ga West District of Ghana. Norsk Geografisk Tidsskrift-Norwegian Journal of Geography, 62(3), pp.210-221..
[9] Muleta, A.J., Lappan, R., Stinear, T.P. and Greening, C., 2021. Understanding the transmission of Mycobacterium ulcerans: A step towards controlling Buruli ulcer. PLoS Neglected Tropical Diseases, 15(8), p.e0009678.
[10] Nienhuis, W.A., Stienstra, Y., Thompson, W.A., Awuah, P.C., Abass, K.M., Tuah, W., Awua-Boateng, N.Y., Ampadu, E.O., Siegmund, V., Schouten, J.P. and Adjei, O., 2010. Antimicrobial treatment for early, limited Mycobacterium ulcerans infection: a randomised controlled trial. The Lancet, 375(9715), pp.664-672.
[11] Chauty, A., Ardant, M.F., Adeye, A., Euverte, H., Guédénon, A., Johnson, C., Aubry, J., Nuermberger, E. and Grosset, J., 2007. Promising clinical efficacy of streptomycin-rifampin combination for treatment of buruli ulcer (Mycobacterium ulcerans disease). Antimicrobial agents and chemotherapy, 51(11), pp.4029-4035.
[12] Etuaful, S., Carbonnelle, B., Grosset, J., Lucas, S., Horsfield, C., Phillips, R., Evans, M., Ofori-Adjei, D., Klustse, E., Owusu-Boateng, J. and Amedofu, G.K., 2005. Efficacy of the combination rifampin-streptomycin in preventing growth of Mycobacterium ulcerans in early lesions of Buruli ulcer in humans. Antimicrobial agents and chemotherapy, 49(8), pp.3182-3186.
[13] Agbo, I.E., Johnson, R.C., Sopoh, G.E. and Nichter, M., 2019. The gendered impact of Buruli ulcer on the household production of health and social support networks: Why decentralization favors women. PLoS Neglected Tropical Diseases, 13(4), p.e0007317.
[14] Bwire, G., Munier, A., Ouedraogo, I., Heyerdahl, L., Komakech, H., Kagirita, A., Wood, R., Mhlanga, R., Njanpop-Lafourcade, B., Malimbo, M. and Makumbi, I., 2017. Epidemiology of cholera outbreaks and socio-economic characteristics of the communities in the fishing villages of Uganda: 2011-2015. PLoS neglected tropical diseases, 11(3), p.e0005407.
[15] Ohene, S.A., Klenyuie, W. and Sarpeh, M., 2016. Assessment of the response to cholera outbreaks in two districts in Ghana. Infectious diseases of poverty, 5(06), pp.71-81.
[16] Zuckerman, J.N., Rombo, L. and Fisch, A., 2007. The true burden and risk of cholera: implications for prevention and control. The Lancet infectious diseases, 7(8), pp.521-530.
[17] World Health Organization, 2010. Cholera vaccines: WHO position paper. Weekly Epidemiological Record= Relevé épidémiologique hebdomadaire, 85(13), pp.117-128.
[18] Osei, F.B., Duker, A.A., Augustijn, E.W. and Stein, A., 2010. Spatial dependency of cholera prevalence on potential cholera reservoirs in an urban area, Kumasi, Ghana. International Journal of Applied Earth Observation and Geoinformation, 12(5), pp.331-339.
[19] Nadri, J., Sauvageot, D., Njanpop-Lafourcade, B.M., Baltazar, C.S., Kere, A.B., Bwire, G., Coulibaly, D., N'Douba, A.K., Kagirita, A., Keita, S. and Koivogui, L., 2018. Sensitivity, specificity, and public-health utility of clinical case definitions based on the signs and symptoms of cholera in Africa. The American journal of tropical medicine and hygiene, 98(4), p.1021.
[20] Ruiz-Moreno, D., Pascual, M., Emch, M. and Yunus, M., 2010. Spatial clustering in the spatio-temporal dynamics of endemic cholera. BMC infectious diseases, 10(1), pp.1-12.

[21] Codeço, C.T., 2001. Endemic and epidemic dynamics of cholera: the role of the aquatic reservoir. BMC Infectious diseases, 1(1), pp.1-14.
[22] Wang, J. and Liao, S., 2012. A generalized cholera model and epidemic–endemic analysis. Journal of biological dynamics, 6(2), pp.568-589.
[23] Eisenberg, M.C., Robertson, S.L. and Tien, J.H., 2013. Identifiability and estimation of multiple transmission pathways in cholera and waterborne disease. Journal of theoretical biology, 324, pp.84-102.
[24] Zhao, J.Q., Bonyah, E., Yan, B., Khan, M.A., Okosun, K.O., Alshahrani, M.Y. and Muhammad, T., 2021. A mathematical model for the coinfection of buruli ulcer and cholera. Results in Physics, 29, p.104746.
[25] Umar, M., Sabir, Z., Raja, M.A.Z., Amin, F., Saeed, T. and Guerrero-Sanchez, Y., 2021. Integrated neuro-swarm heuristic with interior-point for nonlinear SITR model for dynamics of novel COVID-19. Alexandria Engineering Journal, 60(3), pp.2811-2824.
[26] Umar, M., Sabir, Z., Raja, M.A.Z., Baskonus, H.M., Yao, S.W. and Ilhan, E., 2021. A novel study of Morlet neural networks to solve the nonlinear HIV infection system of latently infected cells. Results in Physics, 25, p.104235.
[27] Sabir, Z., Botmart, T., Raja, M.A.Z., Sadat, R., Ali, M.R., Alsulami, A.A. and Alghamdi, A., 2022. Artificial neural network scheme to solve the nonlinear influenza disease model. Biomedical Signal Processing and Control, 75, p.103594.
[28] Sabir, Z., Ali, M.R. and Sadat, R., 2023. Gudermannian neural networks using the optimization procedures of genetic algorithm and active set approach for the three-species food chain nonlinear model. Journal of Ambient Intelligence and Humanized Computing, 14(7), pp.8913-8922.
[29] AbuAli, N., Khan, M.B. and Sabir, Z., 2023. A computational stochastic procedure for solving the epidemic breathing transmission system. Scientific Reports, 13(1), p.16220.
[30] Matlob, M.A. and Jamali, Y., 2019. The concepts and applications of fractional order differential calculus in modeling of viscoelastic systems: A primer. Critical Reviews™ in Biomedical Engineering, 47(4).
[31] Yépez-Martínez, H. and Gómez-Aguilar, J.F., 2019. A new modified definition of Caputo–Fabrizio fractional-order derivative and their applications to the multi step homotopy analysis method (MHAM). Journal of Computational and Applied Mathematics, 346, pp.247-260.
[32] Hong, Y., Liu, Y., Chen, Y., Liu, Y., Yu, L., Liu, Y. and Cheng, H., 2019. Application of fractional-order derivative in the quantitative estimation of soil organic matter content through visible and near-infrared spectroscopy. Geoderma, 337, pp.758-769.
[33] Bonfanti, A., Fouchard, J., Khalilgharibi, N., Charras, G. and Kabla, A., 2020. A unified rheological model for cells and cellularised materials. Royal Society open science, 7(1), p.190920.
[34] Qin, Z., Liu, H.M., Lv, T.T. and Wang, X.D., 2020. Structure, rheological, thermal and antioxidant properties of cell wall polysaccharides from Chinese quince fruits. International journal of biological macromolecules, 147, pp.1146-1155.
[35] Baleanu, D., Sadat Sajjadi, S., Jajarmi, A. and Asad, J.H., 2019. New features of the fractional Euler-Lagrange equations for a physical system within non-singular derivative operator. The European Physical Journal Plus, 134, pp.1-10.
[36] Baleanu, D., Jajarmi, A., Sajjadi, S.S. and Asad, J.H., 2020. The fractional features of a harmonic oscillator with position-dependent mass. Communications in Theoretical Physics, 72(5), p.055002.
[37] Alwabli, Afaf S., Kaci, Abdelhakim, Bellifa, Hichem, Bousahla, Abdelmoumen Anis, Tounsi, Abdelouahed, Alzahrani, D.A., Abulfaraj, A.A., Mahmoud, S.R. "The nano scale buckling properties of isolated protein microtubules based on modified strain gradient theory and a new single variable trigonometric beam theory." Advances in nano research, 10(1), 15-24 (2021).
[38] Alhebshi, A.M.S., Metwally, A.M., Al-Basyouni, K.S., Mahmoud, S.R., Al-Solami, H.M., Alwabli, A.S. "Mechanical Behavior and Physical Properties of Protein Microtubules in Living Cells Using the Nonlocal Beam Theory." Physical Mesomechanics, 25(2), 181-186 (2022).
[39] Benmansour, Djazia Leila, Kaci, Abdelhakim, Bousahla, Abdelmoumen Anis, Heireche, Houari, Tounsi, Abdelouahed, Alwabli, Afaf S., Alhebshi, Alawiah M., Al-ghmady, Khalid, Mahmoud, S.R. "The nano scale bending and dynamic properties of isolated protein microtubules based on modified strain gradient in nano research, 7(6), 443-457 (2019).

[40] Taj, Muhammad, Mohamed A. Khadimallah, Muzamal Hussain, Khurram Fareed, Muhammad Safeer, Khaled Mohamed Khedher, Manzoor Ahmad , S. R. Mahmoud "Thermal stress effects on microtubules based on orthotropic model: Vibrational analysis." Advances in concrete construction 11, no. 3 (2021): 255-260.

[41] Taj, Muhammad, Mohamed A. Khadimallah, Muzamal Hussain, Shaid Mahmood, Muhammad Safeer, Yahya Rashid, Manzoor Ahmad, S. R. Mahmoud "Instability analysis of microfilaments with and without surface effects using Euler theory." Advances in nano research 10, no. 6 (2021): 509-516.

[42] Mahmoud, S. R., Shafeek A. Ghaleb, and A. K. Alzahrani. "Mathematical Model for Study the Microtubules Using Shear Deformation Theories." Applied Mathematical Sciences 11, no. 38 (2017): 1871-1880.

[43] S. R. Mahmoud, Shafeek. A. Ghaleb, A. K. Alzahrani, E. Ghandourah "Mathematical approach of avascular tumor for effect of growth on the mechanical stresses", Applied mathematics and information science, Vol. 11, No. 5, PP:1353-1360, (2017).

[44] Mahmoud, S.R., Al-Solami, H.M., Alkenani, N., Alhebshi, A., Alwabli, A.S., Bahieldin, A. "A mechanical model to investigate Aedes aegypti mosquito bite using new techniques and its applications." Membrane and Water Treatment, 11(6), 399-406 (2020).

[45] Alkenani, Naser, Mahmoud, S.R., Metwally, A.M., Alwabli, A.S., Al-Solami, H.M. "A mechanical approach for mosquito fascicle under the influence of mechanical forces with medical applications." Structural Engineering and Mechanics, 79(6), 677-682 (2021).

[46] Al-Solami, Habeeb M., Alawiah MS Alhebshi, H. Abdo, S. R. Mahmuod, Afaf S. Alwabli, and Naser Alkenani. "A bio-mathematical approach to control the Anopheles mosquito using sterile males technology." International Journal of Biomathematics 15, no. 06 (2022): 2250037.